Recent Trends in the Study of Compact Objects (RETCO-II): Theory and Observation
ASI Conference Series, 2015, Vol. 12, pp 29 – 34
Edited by Indranil Chattopadhyay, Anuj Nandi, Santabrata Das and Samir Mandal

Multi-wavelength studies of Magnetic Cataclysmic Variables

K. P. Singh*
Tata Institute of Fundamental Research, 1 Homi Bhabha Road, Mumbai 400005, INDIA

Abstract. I present a brief review of the present status of multi wavelength emission, from optical to X-rays, from Magnetic Cataclysmic Variables (MCVs). The spectral energy distribution of the MCVs is a perfect match to the multi-wavelength and a very wide X-ray band capabilities of soon to be launched ASTROSAT.

Keywords : accretion – magnetic fields – stars: variables: other – X-rays: binaries

1. Introduction

Magnetic Cataclysmic Variables (MCVs) are semi-detached binary star systems with very short periods, 10 minutes to 10 hours, containing a red dwarf main-sequence-like secondary star and a more massive white dwarf (WD) primary star with a very high magnetic field (B > 10^7 Gauss. The secondary star fills its Roche Lobe and the matter overflows the lobe and is accreted by the primary WD star (see Hameury, King and Lasota,1986; Norton, 1993; Warner, 2003).

Two varieties of MCVs are known: the Intermediate Polars (IPs) or DQ Her stars, and the Polars or AM Her stars. The white dwarfs in the Polars have a magnetic field of 10 - 150 MGauss, whereas the IPs have a lower magnetic field (1 - 10 MG) WD. The accretion in the IPs is via a disrupted accretion disk and an accretion stream or an accretion curtain to the poles of the WD, whereas there is no accretion disk formation in the Polars and accretion is exclusively via an accretion column. The Polars, have short periods, typically less than 2 hrs, and are usually very bright in soft X-rays. The Intermediate Polars are brighter in hard X-rays. The space density of Polars (within

*email: singh@tifr.res.in

the solar neighbourhood of a few kpc) is (3 - 8) $\times$ 10^{-7} pc^{-3}, with the IPs having a volume density of (2 - 5) $\times$ 10^{-7} pc^{-3} (Pretorius, 2014). The X-ray luminosities of MCVs are in the range of 10^{29-33} ergs/s.

2. Multi-wavelength spectra of MCVs

Magnetic CVs emit over a very broad range of wavelengths. Large levels of circular polarisation are seen in the infra-red, optical and UV emission thus implying that the radiation process in these wave bands is largely due to cyclotron emission. The accreted material towards the poles of the WD is de-accelerated and a shock is produced in the flow. The free-falling gas then encounters the shock front where the shock converts the kinetic energy into thermal energy (bulk motion into random motion), thereby releasing most of the gravitational energy in the post-shock region. The resulting shock temperature is given by $T_s = 3GMm_h/8kR$, which is of the order of 10 to 50 keV (M and R being the WD mass and radius respectively). The corresponding X- ray luminosity, $L_X = GMM_\odot/R$, is $\sim 10^{31} - 10^{33}$ erg s^{-1} ($M_\odot$ being the accretion rate). Corresponding hard X-rays are emitted mainly via the bremsstrahlung process and very hot multi-temperature plasma with temperatures reaching several tens of million degrees are also observed along with characteristic atomic lines from the ionised plasma (Girish, Rana, and Singh 2007; Singh 2013, Schlegel et al. 2014). The accreted matter settles down on the surface of the WD. Half of the accreting luminosity illuminates the polar caps and is reprocessed into soft X-rays (> 2 keV) with a characteristic blackbody temperature, $T_{bb} = (L_{acc}/ 8\ f\ \pi R2\sigma)^{1/4}$, $\sim$10−50 eV (f being the irradiated fractional area of the stellar surface). Since the shock occurs very close to the surface of the WD, a significant reflection of bremsstrahlung X-rays can also be expected in the hard X-rays. This is also known as Compton hump due to reprocessing of reflected X-rays. A fluorescent line at 6.4 keV due to Fe-K, is one of the spectral

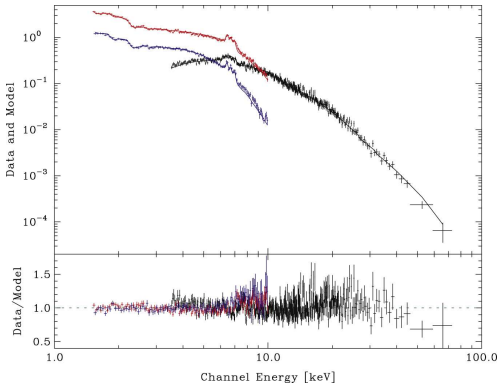

Figure 1. X-ray spectrum of V1223 Sgr as observed with NuStar (black) and XMM MOS (blue) and PN (red) and fitted with a multi-temperature cooling flow model plus Compton reflection. Reproduced with permission from Mukai et al. 2015.

signatures for this, and it has been seen routinely in the X-ray spectra of MCVs (for example, see Girish and Singh 2012). The direct detection of the Compton reflection hump expected to be in the $10 - 30$ keV range has been reported only recently (Mukal et al. 2015) after the availability of sensitive observations with NuStar at high energies (See Figure 1). The presence of complex accretion patterns like curtains also lead to partial and variable absorption in the soft X-rays (Rana et al. 2005, Girish and Singh 2012). All these features combined with the spin and orbital modulations of the MCVs make simultaneous studies across all the emission regions essential to fully understand these systems and their behaviour. An example of the multi wavelength spectrum of a Polar is shown in Beuremann (1998) [also reproduced in Singh (2013)].

The UV spectra of MCVs show a large number of emission lines from multiple species of He II, carbon, oxygen and magnesium lines at λ 1335, 1371, 1393/1402, 1550, 1640, 2297, 2386, 2733, 2800, 3133 and 3203 Angstroms. An example of such a rich spectrum can be seen in Shrader, Singh and Barrett (1997) who have listed the ratio of the line strengths for the He lines at λ2733 in NUV to 1640 Angstroms in FUV for several MCVs and compared them to the strength of the X-ray emission but failed to find any correlation probably due to limited temporal sampling. They, however, were able to constrain the size and thermodynamics of the emitting region using the well known relation between He II Lyα and the oxygen lines produced by the Bowen fluorescence mechanism seen in the Polar RX J1802.+1804.

3. ASTROSAT and its capabilities for the study of MCVs

ASTROSAT is India's first astronomy satellite with multi-wavelength (visible, near UV, far UV and X-rays) capability to be launched in the last quarter of 2015 (Singh et al. 2014). It has a very wide X-ray band spanning from 0.3 to 100 keV covered by three instruments: a soft X-ray imaging telescope (SXT) in $0.3 - 8.0$ keV energy band, three large area Xe-filled proportional counters (LAXPCs), and CdZnTe Imager (CZTI) with a coded mask together covering the hard X-ray every band of $3 - 100$ keV. The sensitivity of the SXT is comparable to that of the *Swift-XRT*, whereas the CZTI is factor 4 lower in area when compared to the *Swift- BAT*. The three LAXPC units combined have much larger area than the *RXTE* and also cover a much wider energy range of $3 - 80$ keV making them the most sensitive large area proportional counters ever flown in this energy band. A simulation of the x-ray spectrum expected to be seen in a 50 kilo-sec observation of a well known IP, V1233 Sgr, with the ASTROSAT X-ray instruments is shown in Figure 2. The broad energy band of co-aligned X-ray instruments would allow the detection of Compton reflection from sources like V1223 Sgr as is shown in Figures 3 and 4. Here, we have first simulated the X-ray spectrum as would be seen by ASTROSAT based on the spectral measurements by XMM and NuStar (Mukai et al. 2015), and shown a) the reflection component in the residuals by removing that component alone in Fig. 3, and then b) refitting with the same model as used in Mukai et al (2015) but by varying the param-

eters and without including the reflection component in Fig. 4. The residuals in Fig. 4 clearly show that the simulated data cannot be fit without adding the reflection component. The reduced chi-square values go from 0.96 to 2.16 for fit with and without the reflection component. This shows that even smaller contributions of the reflection component than observed in V1223 Sgr would be detectable with ASTROSAT. ASTROSAT's ultra-violet imaging telescope (UVIT) has a total of 13 filters in the FUV (130 - 180 nm), NUV (200 - 300 nm), and VIS (320 - 550 nm) wavelength ranges, and gratings in the two main ultraviolet channels for low resolution (100) slit-less spectroscopy (Singh et al. 2014). Long exposures and extensive sampling with the ASTROSAT will be able to detect several of the strong lines from the MCVs with the gratings simultaneous with the X-ray observations and provide the diagnostics for the emission regions and how they respond to the various X-ray components. The sensitivity of ASTROSAT across all the bands from optical, NUV, FUV to hard X-rays makes it a very useful instrument to study the multi-wavelength emission from MCVs simultaneously. As an example the FUV spectra of AM Her expected based on its IUE spectrum is shown in Figure 5.

Acknowledgements

I thank V. Girish (ISAC, Bengaluru) and S. Annapurni (IIA, Bengaluru) for the X-ray and FUV simulations, respectively, with the ASTROSAT instruments shown in this paper. I thank Koji Mukai and his co-authors for allowing the reproduction of a figure from their recent paper.

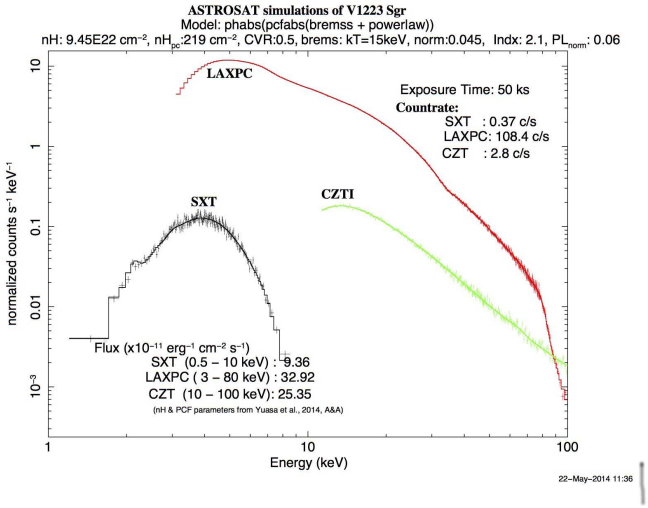

Figure 2. Simulated X-ray spectrum of V1223 Sgr expected to be observed with the broad energy band of ASTROSAT.

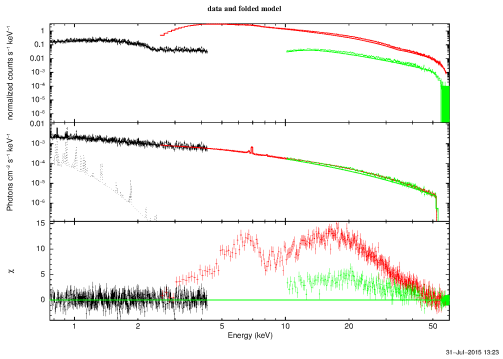

Figure 3. Simulated X-ray spectrum of V1223 Sgr with the inclusion of a reflection component as reported by Mukai et al.(2015) in the ASTROSAT. The histogram fit to the data does not include the reflection component, and thus the residuals show the strength of the reflection component. The black, red and green colours refer to SXT, LAXPC and CZTI respectively.

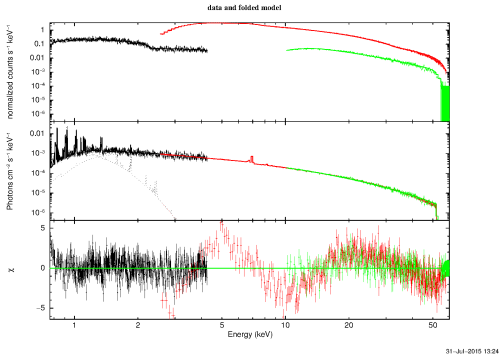

Figure 4. Simulated X-ray spectrum of V1223 Sgr with ASTROSAT as in Fig 3. The histogram fit to the data again does not include the reflection component but parameters of the rest of the continuum are now varied to fit the data without invoking the reflection. The residuals indicate that the fit is poor without reflection.

References

Beuermann K., 1999, in Aschenbach B., Freyberg M. J., eds, Proc. Highlights in X-ray astronomy, June 17-19, 1998, Garching, Germany, MPE report No. 272, ISSN 0178-0719, p. 410.

Girish V., Rana V. R., Singh K. P., 2007, ApJ, 658, 525

Girish V., Singh K. P., 2012, MNRAs, 427, 458.

Hameury J. R., King A. R., Lasota J. P., 1986, MNRAS, 218, 695.

Mukai K., Rana V., Bernardini F., de Martino D., 2015, ApJ, 807, L30.

Norton A. J., 1993, MNRAS, 265, 316.

Pretorius M. L., 2014, in The X-ray Universe 2014, Dublin, edited by Jan-Uwe Ness.

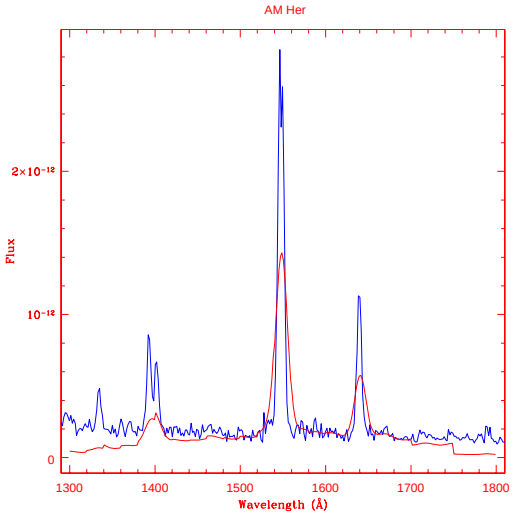

Figure 5. Simulated spectrum (red colour) of AM Her expected to be observed with the ASTROSAT's low resolution grating in the FUV band, based on the IUE spectrum shown in blue colour.

Rana V. R., Singh K. P., Barrett P., Buckley D. A. H., 2005, ApJ, 625, 351

Schlegel E. M., Shipley H. V., Rana V. R., Barrett P. E., Singh K. P., 2014, ApJ., 797, 38.

Sharder C. R., Singh K. P., Barrett P.,1997, ApJ, 486, 1006.

Singh K. P., 2013, in Das S., Nandi A., Chattopadhyay I., eds, Recent Trends in the Study of Compact Objects: Theory and Observation ASI Conference Series, 8, 115.

Singh K. P., et al., 2014, Proc. of the S.P.I.E. Conference 9144 on Space Telescopes and Instrumentation 2014: Ultraviolet to Gamma Ray", June 22 - 27, 2014, Montreal, Ref. No. 9144-63.

Rautela B. S., Joshi G. C., Pandey J. C., 2004, BASI, 32, 159

Warner B., 2003, Cataclysmic Variable Stars, Cambridge Univ. Press, Cambridge, p. 592